Altruism, Social Interactions, and the Course of a Pandemic*

Laura Alfaro†
Harvard Business School and NBER

Ester Faia‡
Goethe University Frankfurt and CEPR

Nora Lamersdorf§
Frankfurt School of Finance & Management

Farzad Saidi¶
University of Bonn and CEPR

April 11, 2023

Abstract

Externalities and social preferences, such as altruism, play a key role in the choice of social interactions, which in turn affect the diffusion of a pandemic. We build a dynamic epidemiological model with endogenous social interactions in a frictional environment, also in a variant with heterogeneous agents and a network structure. Taking into account agents' endogenous behavior and altruism generates markedly different predictions relative to a naïve epidemiological model with exogenous contact rates. Congestion and commitment inefficiencies arise, even under full altruism, and call for policy intervention. We derive the efficient allocation, and show how the Ramsey planner can mitigate the respective externalities.

JEL codes: D62, D64, D85, D91, E70, I10, I18

Keywords: social interactions, pandemics, SIR models, social preferences, targeted policies

∗ We thank John Cochrane, Pietro Garibaldi, Maximilian Mayer, Krisztina Molnar, Dirk Niepelt, Vincenzo Pezone and Venky Venkateswaran, as well as multifarious seminar participants for their comments and suggestions. We also thank Christina Brinkmann for excellent research assistance. Saidi's research is funded by the Deutsche Forschungsgemeinschaft (DFG, German Research Foundation) under Germany's Excellence Strategy (EXC 2126/1 – 390838866), and Faia gratefully acknowledges funding by the DFG under grant FA-1022-2. A previous version of the model was circulated as NBER Working Paper No. 27134 under the title "Social Interactions in Pandemics: Fear, Altruism, and Reciprocity."
† E-mail: lalfaro@hbs.edu
‡ E-mail: faia@wiwi.uni-frankfurt.de
§ E-mail: n.lamersdorf@fs.de
¶ E-mail: saidi@uni-bonn.de

1. Introduction

Externalities, positive or negative, may arise naturally in networked communities. Furthermore, societies and cultures exhibit deeply rooted differences in traits such as social preferences (see, among others, Hofstede, 2001; Spolaore and Wacziarg, 2013; Falk et al., 2018). Both affect individuals' choice of social interactions, which in turn governs the extent of network externalities, such as the diffusion of information or an infectious disease. However, these phenomena have mostly been studied in models with exogenous contact rates that neglect behavioral adjustments. The goal of this paper is to build a framework that incorporates these behavioral adjustments and to design the optimal policy response, taking into account different community and social traits.

We build a dynamic model in which agents choose the intensity of social interactions. In a frictional environment, they maximize their lifetime utility, which increases with social contacts, while internalizing potential externalities stemming from these social contacts. When agents are altruistic, they also take into account the impact of their behavior on others. We apply our model to the COVID-19 pandemic. The standard SIR[1] model, the primary toolkit for predicting the spread of viral diseases since the 1920s, assumes that contacts—and, as such, infection probabilities—among agents are exogenous and immutable even as awareness of the infection risk and its harm on others increases. However, human beings react to risk, policy decisions, and also to the decisions of others. If model solutions neglect such behavioral adjustments, policy responses that are built on them are most likely misguided. In contrast to the classical SIR models, in ours agents optimally choose their social contacts. Hence, their behavior directly affects the spread of the disease.

We provide a theoretical rationale for the role of social preferences in facilitating the internalization of health externalities, such as those during the COVID-19 pandemic. We show that susceptible individuals, aware of their infection risk, voluntarily reduce their social contacts. The decision problems of the agents are framed in a frictional context with

1 SIR stands for "S," the number of susceptible, "I," the number of infectious, and "R," the number of recovered, deceased, or immune individuals.

an underlying matching process for the chosen social intensity.[2] The intensity of social interactions determines the infection probability and, thus, the evolution of the number of susceptible, infected, and recovered individuals. Agents take as given the shocks and the aggregate states of the disease. We find that their behavioral adjustment flattens the infection curve compared to a model with exogenous contact rates, even in the absence of any stringency measures imposed by a social planner.

Motivated by the empirically documented importance of altruism in reducing mobility during the pandemic (Alfaro et al., 2022), we follow Becker (1974) and include an altruistic motive in the lifetime utility of infected individuals,[3] such that they care about the infection risk of their susceptible peers and change their own behavior accordingly. Using simulations, we show that a higher degree of altruism helps significantly flatten the infection curve. This is the net outcome of two effects: while altruistic infected agents reduce their social contacts by more, this also allows susceptible agents to decrease their social activity by less due to the lower infection risk stemming from a reduction of infected agents' social contacts.

We also present a network variant of our model with different groups among the susceptible, infected, and recovered. These groups represent individuals who are heterogeneously exposed to the infection risk due to different recovery rates. In this model variant, agents from a given group choose the level of social interactions towards all groups individually. In simulations, we illustrate that susceptible individuals belonging to a more vulnerable group reduce their overall social activity by more, and especially so towards members from a potentially more infectious group. Altruistic infected individuals, in turn, reduce their social interactions by more towards members from a more vulnerable group. Again, a higher degree of altruism gives susceptible agents—especially the more vulnerable ones—the possibility to reduce their social interactions by less since part of the burden is carried by the infected agents.

By comparing the decentralized and the social planner's solution of our model, we show that congestion and commitment inefficiencies arise in the former. The (static) congestion inefficiency is dictated by the non-linearities of the matching process and the (dynamic)

2 See Diamond (1982) and Petrongolo and Pissarides (2001) for an overview.

3 This enables us to yield a time-consistent solution to our dynamic problem (as in, for instance, Doepke and Tertilt, 2009).

commitment inefficiency by the failure of atomistic agents to foresee the aggregate future evolution of the disease, which the planner is well aware of.[4] Inefficiencies, in turn, call for policy intervention. As in the SIR-network model inefficiencies are specific to groups, addressing them requires group-targeted policies. From the range of potential policy instruments, we focus on lockdowns, a prominent "corner solution" during the earlier waves of the pandemic. We characterize under what conditions such a stringency policy can achieve efficiency by equalizing the ratio of the marginal utility from social activity for an infected agent and the one for a susceptible agent across the decentralized equilibrium and the efficient solution.

Finally, we quantify the optimal lockdown policy through the simulation of a Ramsey plan, in which the policymaker enforces an instrument by taking into account all agents' optimizing conditions. A distinctive feature of the Ramsey lockdown plan is its front-loading, as most of the activity is restricted in the first few periods. In the SIR-network model with heterogeneous agents, we show that optimal initial restrictions are stricter for agents that spread the disease more, and later restrictions are stricter for the most vulnerable groups.

Relation to the literature. Our paper contributes to the emerging and expanding literature on health externalities and their social consequences. Following the pandemic, there has been increasing recognition of the role of endogenous behavior in the face of those externalities. The key novelty of our paper lies in examining how social preferences and other behavioral elements shape social interactions in an endogenous network, including its comparison with a social planner internalizing externalities.

More generally, our paper contributes to the long-standing literature on other-regarding preferences. Pro-social behavior and, specifically, altruism have been studied in several forms, ranging from warm-glow preferences to unconditional altruism (see Becker, 1974; Andreoni, 1989, 1993; Bolton and Ockenfels, 2000; Andreoni and Miller, 2002; Frey and Meier, 2004). In the context of pandemics, Casoria et al. (2023) show that prosocial preferences remained stable during the recent COVID-19 pandemic. In a companion paper, Casoria et al. (2021) explore the interplay between laws and social norms during the same period. Prosocial preferences

4 This is similar to Moser and Yared (2022), in that we highlight dynamic inefficiencies compared to the social planner's commitment.

have important implications for our setting: the fact that infected individuals internalize the cost of infection for susceptible individuals and reduce their contacts accordingly allows the latter to reduce their social interactions by less. Our comparison with the social planner's solution highlights a difference in social interactions that may emerge even when all agents exhibit the maximum degree of altruism, to our knowledge a novel result in the literature.

While we devise an application to the pandemic, our theory contributes to the literature on endogenous network formation and, in particular, to a class of models in which agents make a costly contact-intensity choice in a frictional market. There are prominent applications of these models to goods markets (see Rubinstein and Wolinsky, 1987) or financial markets (see Duffie et al., 2005; or, more recently, Farboodi et al., 2023). Closer to ours are models that study endogenous social-network formation within a search-theoretical framework. In this vein, work on social capital goes back to Becker (1996). Endogenous social interactions were first formalized in an equilibrium model by Brock and Durlauf (2001). Fortin et al. (2007) study the role of endogenous social interactions in the context of tax evasion. The impact of social interactions on neighborhoods or social structures is covered by Case and Katz (1991) and Glaeser et al. (1996). An important feature of our model is that it includes a role for altruism which further shapes interactions in the presence of negative externalities on others. In addition, we allow for groups that are heterogeneous in their vulnerability to the externalities.

Closely related to our model is that by Currarini et al. (2009), who study the formation of social ties through utility maximization, and show the emergence of homophily through a biased search and matching process. Cabrales et al. (2011) provide a tractable model where both socialization (or network formation) and productive efforts can be analyzed simultaneously. Their model adopts a quadratic payoff function and allows to derive a tractable welfare criterion. In our framework, agents solve dynamic optimization problems where payoff functions are concave. As such, our paper also relates to the literature on informal insurance in random and social networks, which studies how transfers and obligations translate into risk sharing (see Bramoullé and Kranton, 2007; Bloch et al., 2008; Ambrus et al., 2014).

The literature on the economics of pandemics has evolved fast and now comprises a substantial body of work. Any feasible list would be incomplete at this point, so we focus on the papers directly related to ours. One notion that has gained ground is the fact that any model, even one with heterogeneous agents, might have low predictive power and lead to naïve policy prescriptions when neglecting the role of agents' reactions and social preferences. Kremer (1996) is one of the first studies to integrate behavior in an epidemiological model. More recently, among the papers that address this issue independently, also in a search-theoretical context, are Garibaldi et al. (2020a,b), Farboodi et al. (2021), Brotherhood et al. (2020), Chakrabarti et al. (2022), and Dasaratha (2022). All of these papers highlight the role of infection externalities associated with contact exposure to infected individuals.

Unlike Garibaldi et al. (2020a,b) and Farboodi et al. (2021), we differentiate between the behavior of susceptible and infected individuals, include a role for altruism, and formalize the endogenous social network, and its social planner solution, with heterogeneous groups.[5] Chakrabarti et al. (2022) and Dasaratha (2022) focus on the interaction of behavioral adjustments and policies during the pandemic. While the former paper points out the important role of testing as a policy instrument, the latter shows that behavioral responses can, under certain circumstances, lead to paradoxical effects of policy interventions. Brotherhood et al. (2020) study the spread of the pandemic in a model that includes an altruistic motive for infected individuals, and distinguish between old and young age groups. However, they model altruism as an additional constant preference parameter for staying at home in the utility function of infected individuals. In our model, the utility of altruistic infected individuals depends directly on that of susceptible individuals, leading the former to internalize the externalities of their behavior at each point in time depending on the current states and behavior of others.

Importantly, we propose a variant with heterogeneous agents and an endogenous network structure, in which agents of each group of the population choose their social interactions vis-à-vis each other group.[6] Analyzing different agents that are heterogeneous, e.g., with

5 Another difference with Farboodi et al. (2021) is that we adopt a discrete-time version of a search-theoretical framework and carve out the role of the dynamic inefficiency.

6 A notable exception is Wu and Shimer (2021), who apply an endogenous network model to the pandemic without an altruistic motive but analyzing strategic complementarities in matching.

respect to age, is crucial in the context of a pandemic that imposes different costs on different types of agents (see, e.g., Gollier, 2020, for a cost-benefit analysis of age-specific lockdowns). Acemoglu et al. (2021) study the spread of the pandemic in a network with heterogeneous groups, but links are exogenous and social preferences are absent. In our model, altruistic infected individuals reduce their contacts by more towards members of a more vulnerable segment of the population. This contributes to a greater flattening of the infection curve than is the case in Acemoglu et al. (2021). Our model adds the role of social preferences and the design and numerical solution of the social planner's solution to an endogenous network model.

2. A Model of Endogenous Social Interactions and Altruism

In this section, we first outline the dynamic optimization problem in the homogeneous SIR model and then extend it to the network variant. The decentralized solutions of the two models are followed by the efficient planner's solutions, on the basis of which we discuss the design of an optimal lockdown policy.

2.1. Dynamic Optimization

Model setup. In our model, time is discrete, and there is an infinite horizon. Individuals are in one of the following three states: susceptible (S), infected (I), or recovered (R). Susceptible agents are all equally exposed to infection risk. Transitions of susceptible individuals from state S to I depend on contacts with other people which can arise in, e.g., entertainment activities, other outside activities, or the workplace.[7]

Each representative agent has an additively separable per-period utility function $U(x^i_{h,t}, x^i_{s,t}) = u(x^i_{h,t}, x^i_{s,t}) - c(x^i_{h,t}, x^i_{s,t})$, where $x^i_{h,t}$ denotes home activities and $x^i_{s,t}$ social activities at time t and $i \in \{S, I, R\}$. $u(x^i_{h,t}, x^i_{s,t})$ is increasing in its arguments and the cost function, $c(x^i_{h,t}, x^i_{s,t})$,

7 Transitions of individuals in the infected group, I, to recovery, R, depend only on medical conditions related to the disease (mostly the healthcare system) that are outside of an individual's control.

puts a constraint on the choice of home and social activities. We assume that the per-period utility function is concave with $\frac{\partial^2 U(x^i_{h,t}, x^i_{s,t})}{\partial^2 x^i_{s,t}} < 0$.

At time t, a susceptible agent enjoys the per-period utility, expects to enter the infected state in the next period with probability p_t or to remain susceptible with probability $(1 - p_t)$, and chooses the amount of home and social activities. In doing so, she recognizes that her own social activity increases the risk of infection, taking as given the average social activity of others and the aggregate states of the disease. The value function of a susceptible individual reads as follows:

$$V^S_t = U(x^S_{h,t}, x^S_{s,t}) + \beta[p_t V^I_{t+1} + (1 - p_t)V^S_{t+1}], \tag{1}$$

where β is the time discount factor and captures the agent's degree of patience, and V^I_t is the value function of an infected individual. The latter is given by:

$$V^I_t = U(x^I_{h,t}, x^I_{s,t}) - C^I + \beta[(1 - \gamma)V^I_{t+1} + \gamma V^R_{t+1}] + \delta S_t V^S_t, \tag{2}$$

where C^I is a cost that individuals incur while being infected. Infected individuals remain so for an additional period with probability $(1 - \gamma)$ or recover with probability γ. They might care about their susceptible peers, of which there are S_t. Therefore, the parameter δ captures the degree of altruism and puts a weight on the lifetime utility of susceptible individuals, multiplied by their population share.[8] In line with Garibaldi et al. (2020a), we assume that the lifetime utility of infected individuals is lower than that of susceptible individuals, giving the latter an incentive to avoid an infection:[9]

Assumption 1. $V^I_t - V^S_t < 0 \ \forall t$.

The value function of recovered individuals reads as follows:

$$V^R_t = U(x^R_{h,t}, x^R_{s,t}) + \beta V^R_{t+1}, \tag{3}$$

8 Such a setup implicitly assumes that agents recognize their symptoms. As known, there are also asymptomatic cases. However, extending our model to incorporate the latter would not affect the main channels that we discuss.

9 Note that one can choose a combination of parameter values (the infection cost C^I, the recovery rate γ, the degree of altruism δ, and the disease transmission rate η) such that this assumption will be fulfilled.

as once they have recovered, they are immune to a new infection.

The contact probability p_t determines the infection rate in the classical SIR system:

$$S_{t+1} = S_t - p_t S_t \tag{4}$$

$$I_{t+1} = I_t + p_t S_t - \gamma I_t \tag{5}$$

$$R_{t+1} = R_t + \gamma I_t, \tag{6}$$

where S_t, I_t, and R_t denote the total share/number of susceptible, infected, and recovered individuals, respectively, at time t and $S_t + I_t + R_t = N_t \equiv 1 \; \forall t$.

Note that the exogenous contact rate in the classical SIR model, which is presented in Appendix E where we also briefly describe its limitations, relates to our infection probability as follows: $p_t = \lambda I_t$, where λ is assumed to be constant and exogenously given.

Matching function, geography, and infection probability. The number of contacts per individual depends on a matching process along the lines of Diamond (1982) or Pissarides (2000), which captures the role of congestion externalities such as those due to urban density. In this context, the intensity of an individual's social interactions, $x^i_{s,t}$ for $i \in \{S, I, R\}$, can be defined as the number of times she leaves her home or the probability of doing so per unit of time. In the course of these social activities, agents come in contact with other individuals. The number of contacts depends on the average level of social activity in the population, $\bar{x}_{s,t}$. Normalizing the population size to 1, the latter is given by $\bar{x}_{s,t} = S_t \bar{x}^S_{s,t} + I_t \bar{x}^I_{s,t} + R_t \bar{x}^R_{s,t}$, where $\bar{x}^S_{s,t}$, $\bar{x}^I_{s,t}$, and $\bar{x}^R_{s,t}$ are the average levels of social activity of susceptible, infected, and recovered individuals, respectively.

The total number of contacts for the average level of social activity depends on the matching function $m(\bar{x}_{s,t}) = (\bar{x}_{s,t})^\alpha$. The parameter α captures the returns to scale, which serves as a proxy for geographical properties. Cities with denser logistical structures induce more overall contacts per social activity. The average number of contacts per social activity is then given by $\frac{m(\bar{x}_{s,t})}{\bar{x}_{s,t}} = (\bar{x}_{s,t})^{\alpha-1}$. Since each susceptible individual chooses at each point in time the amount of social activities depending on her preferences, we multiply the average

number of contacts per social activity with the susceptible individual's chosen level of social activity. Hence, the overall number of contacts of a susceptible agent equals $x^S_{s,t}(\bar{x}_{s,t})^{\alpha-1}$.

To determine the infection probability, we need to account for the extent to which the social contacts of a susceptible individual are with infected individuals. This depends, on the one hand, on the number of agents who are infected, I_t. On the other hand, also infected individuals choose their level of social activity, $x^I_{s,t}$, endogenously. Therefore, we multiply the number of infected individuals I_t with the level of their social activity $x^I_{s,t}$. In sum, the infection probability in the decentralized equilibrium is given by

$$p_t(\cdot) = \eta x^S_{s,t} x^I_{s,t} \frac{m(\bar{x}_{s,t})}{\bar{x}_{s,t}} I_t = \eta x^S_{s,t} x^I_{s,t} (\bar{x}_{s,t})^{\alpha-1} I_t, \tag{7}$$

where $\eta > 0$ is an exogenous transmission rate. If $\alpha = 0$, the probability $p_t = \eta x^S_{s,t} x^I_{s,t} \bar{x}^{-1}_{s,t} I_t$ is homogeneous of degree one, implying constant returns to scale, while if $\alpha = 1$, the probability becomes a quadratic function (see Diamond, 1982), exhibiting increasing returns to scale. Note that atomistic agents take the level of social interactions of other agents as given.

Optimality conditions. Susceptible individuals' first-order conditions with respect to $x_{h,t}$ and $x_{s,t}$ are as follows:

$$\frac{\partial U(x^S_{h,t}, x^S_{s,t})}{\partial x^S_{h,t}} = 0; \qquad \frac{\partial U(x^S_{h,t}, x^S_{s,t})}{\partial x^S_{s,t}} + \beta \frac{\partial p_t(\cdot)}{\partial x^S_{s,t}} (V^I_{t+1} - V^S_{t+1}) = 0. \tag{8}$$

Home activities $x_{h,t}$ do not influence the probability of infection. Therefore, in our model, their level does not change during the pandemic.[10] In contrast, susceptible individuals internalize the drop in utility associated with the risk of infection and—given Assumption 1 and the shape of the utility function—choose a lower level of social activity than they would in the absence of a pandemic. In line with empirical evidence in Alfaro et al. (2022), a higher

10 This modeling choice is chosen for simplicity rather than realism. However, allowing also home activities to change during the pandemic would not affect our qualitative results for social activities.

discount factor β, capturing a higher level of patience, curbs social activity by more. The first-order conditions of infected agents with respect to $x_{h,t}$ and $x_{s,t}$ are as follows:

$$\frac{\partial U(x^I_{h,t}, x^I_{s,t})}{\partial x^I_{h,t}} = 0; \quad \frac{\partial U(x^I_{h,t}, x^I_{s,t})}{\partial x^I_{s,t}} + \delta S_t \beta \frac{\partial p_t(\cdot)}{\partial x^I_{s,t}}(V^I_{t+1} - V^S_{t+1}) = 0. \tag{9}$$

Finally, the first-order conditions of the recovered individuals are: $\frac{\partial U(x^R_{h,t}, x^R_{s,t})}{\partial x^R_{h,t}} = 0$; $\frac{\partial U(x^R_{h,t}, x^R_{s,t})}{\partial x^R_{s,t}} = 0$. Recovered individuals, assuming that they are immune to another infection, choose the same level of social activity as they would in the absence of a pandemic. In contrast to recovered individuals, susceptible and altruistic infected ones have incentives that involve a dynamic component, which depends on the infection risk.

Definition 1. *A decentralized equilibrium is a sequence of state variables S_t, I_t, R_t, a set of differentiable and bounded value functions V^S_t, V^I_t, V^R_t, an infection probability p_t, and a sequence of home consumption and social activities $x^S_{h,t}, x^I_{h,t}, x^R_{h,t}, x^S_{s,t}, x^I_{s,t}, x^R_{s,t}$ such that:*

1. *S_t, I_t, R_t solve* (4)-(6)*, with the probability of infection given by* (7)*.*
2. *V^S_t, V^I_t, V^R_t solve* (1)-(3)*.*
3. *The sequence $p_t, x^S_{h,t}, x^I_{h,t}, x^R_{h,t}, x^S_{s,t}, x^I_{s,t}, x^R_{s,t}$ solves* (8)*,* (9)*, as well as $\frac{\partial U(x^R_{h,t}, x^R_{s,t})}{\partial x^R_{h,t}} = 0$, $\frac{\partial U(x^R_{h,t}, x^R_{s,t})}{\partial x^R_{s,t}} = 0$.*

Note that underlying the decentralized economy is a symmetric Nash equilibrium in the choice of social activity.

The role of altruism. Infected individuals internalize the impact of their decisions on the infection risk for others based on their degree of altruism, which is given by $\delta \in [0, 1]$. If the latter is 0, infected individuals do not internalize the effects of their activity on others, and their first-order condition becomes $\frac{\partial U(x^I_{h,t}, x^I_{s,t})}{\partial x^I_{s,t}} = 0$. In this case, given the concavity of the utility function and Assumption 1, their level of social activity is higher than the one solving (9) with $\delta > 0$. Since the level of social activity of the infected individuals affects the overall infection rate, their degree of altruism is crucial in determining the overall disease transmission and affects the behavior of susceptible individuals. The following proposition formalizes this finding.

Proposition 1. *Social activity of infected individuals, $x^I_{s,t}$, declines with the degree of altruism, and social activity of susceptible individuals, $x^S_{s,t}$, increases with it.*

Proof. See Appendix A.1.

If infected individuals behave more cautiously due to altruism, the infection probability falls, allowing susceptible individuals to have more social interactions. In addition, in Section 3, we show that the presence of altruism leads to a lower number of infected individuals overall, thereby flattening the infection curve.

2.2. Extension to an Endogenous Network Model

Within communities, there are heterogeneous groups that differ along several dimensions and interact with one another. Individuals of each one of these groups optimally choose their level of social interactions vis-à-vis their own and any other group, taking as given the actions of others. This extends the notion of a Nash equilibrium to the entire network. In this framework, interactions are again fully endogenous and depend on the states (S, I, R) within each group and the actions of others.[11]

Applying our analysis to the recent pandemic, we assume that groups differ in terms of their recovery rates, γ^j, which can vary, for instance, across age groups. Each susceptible individual of group j experiences a certain number of contacts per social activity with infected individuals of her own group but also of the other groups. We denote by $\hat{x}^j_{s,t}$ group j's social interactions at time t. The matching function for each group j reads as follows: $m^j(\hat{x}^j_{s,t}) = \left(\sum_k (\bar{x}^{S,jk}_{s,t} + \bar{x}^{I,jk}_{s,t} + \bar{x}^{R,jk}_{s,t})(\bar{x}^{S,k}_{s,t} S^k_t + \bar{x}^{I,k}_{s,t} I^k_t + \bar{x}^{R,k}_{s,t} R^k_t)\right)^{\alpha}$, where $\bar{x}^{S,jk}_{s,t}$, $\bar{x}^{I,jk}_{s,t}$, and $\bar{x}^{R,jk}_{s,t}$ are the respective average intensities of social activity between (each) group j and group k with $k = 1, ..., J$ and $\bar{x}^{i,k}_{s,t} = \sum_j \bar{x}^{i,kj}_{s,t}$ for $i \in \{S, I, R\}$.

The probability of infection for a susceptible person in group j who comes in contact with infected individuals in all groups k is $p^j_t(\cdot) = \sum_k \eta x^{S,jk}_{s,t} x^{I,kj}_{s,t} \frac{m^j(\hat{x}^j_{s,t})}{\hat{x}^j_{s,t}} I^k_t$. The dynamics of the different states S, I, and R are as described above, but now separately for each group, where

11 Appendix F presents an intermediate version of the model in which optimizing agents choose the general level of social activity, while the cross-group links are exogenous.

now $S_t^j + I_t^j + R_t^j = N_t^j$ and $\sum_j N_t^j \equiv 1 \; \forall t$. The first-order condition for the social activity of susceptible individuals belonging to group j vis-à-vis group k is:

$$\frac{\partial U(x_{h,t}^{S,j}, x_{s,t}^{S,jk})}{\partial x_{s,t}^{S,jk}} + \beta\eta x_{s,t}^{I,kj} \frac{m^j(\hat{x}_{s,t}^j)}{\hat{x}_{s,t}^j} I_t^k (V_{t+1}^{I,j} - V_{t+1}^{S,j}) = 0. \tag{10}$$

Note that now we have J^2 such first-order conditions.

Similarly, for infected individuals with altruistic preferences, the first-order condition with respect to social interactions of each such individual j with agents in any other group k is:

$$\frac{\partial U(x_{h,t}^{I,j}, x_{s,t}^{I,jk})}{\partial x_{s,t}^{I,jk}} + \delta \frac{S_t^k}{N_t^k} \beta\eta x_{s,t}^{S,kj} \frac{m^k(\hat{x}_{s,t}^k)}{\hat{x}_{s,t}^k} I_t^j (V_{t+1}^{I,k} - V_{t+1}^{S,k}) = 0. \tag{11}$$

The first-order conditions for social interactions of the recovered individuals are the same as in the baseline model, but separately for each group j vis-à-vis each group k.

Definition 2. *A decentralized equilibrium for the SIR-network model with a differential choice of group interactions is equivalent to Definition 1, but for each group j of the population. The J^2 equations* (10) *and* (11) *replace the previous first-order conditions* (8) *and* (9) *and the J^2 equations $\frac{\partial U(x_{h,t}^{R,j}, x_{s,t}^{R,jk})}{\partial x_{s,t}^{R,jk}} = 0$ replace $\frac{\partial U(x_{h,t}^{R}, x_{s,t}^{R})}{\partial x_{s,t}^{R}} = 0$.*

Corollary 1. *Social activity of susceptible agents of group j vis-à-vis any group k is smaller if there are many infected agents in group k.*

Proof. From the first-order condition (10) it becomes clear that with $V_{t+1}^{I,j} - V_{t+1}^{S,j} < 0$, a larger I_t^k—given the social activity of infected agents $x_{s,t}^{I,kj}$ and the average social activities—leads to a larger marginal utility $\frac{\partial U(x_{h,t}^{S,j}, x_{s,t}^{S,jk})}{\partial x_{s,t}^{S,jk}}$. Due to the concavity of the utility function, this leads to a decrease in $x_{s,t}^{S,jk}$.

Intuitively, if an individual of group j is aware that in group k the share of infected individuals is high, it will reduce the contact with members of that group in order to avoid infection.

Corollary 2. *Social activity of altruistic infected agents of group j vis-à-vis any group k is smaller if the recovery rate of agents in group k is smaller.*

Proof. Suppose there are two agents, k and k', with different recovery rates, $\gamma^k < \gamma^{k'}$. Agent k, hence, remains longer in the infected state, paying the infection cost, so that $V_t^{I,k} - V_t^{S,k} < V_t^{I,k'} - V_t^{S,k'}$. Therefore, the second term in equation (11) is smaller for social interactions with agents of group k, implying a higher marginal utility, $\frac{\partial U(x_{h,t}^{I,j}, x_{s,t}^{I,jk})}{\partial x_{s,t}^{I,jk}} > \frac{\partial U(x_{h,t}^{I,j}, x_{s,t}^{I,jk'})}{\partial x_{s,t}^{I,jk'}}$, and a lower level of social activity vis-à-vis agents of group k, $x_{s,t}^{I,jk} < x_{s,t}^{I,jk'}$.

Corollary 2 states that altruistic infected agents behave more cautiously towards susceptible agents of a more vulnerable group. We further validate our findings using simulations in Section 3.

2.3. Social Planner

In the decentralized equilibrium, each individual takes as given the average level of social activity and the future course of the number of susceptible and infected individuals. In contrast, a social planner takes both into account when deciding on her policies. We now draw the comparison between the decentralized equilibrium and the solution to the planner's problem for both models described above.

Baseline model. There is complete information, and the planner knows that in a Nash equilibrium each agent in state i chooses the same amount of social activities, so that $x_{s,t}^i = \bar{x}_{s,t}^i$ for $i \in \{S, I, R\}$. The equilibrium infection rate is then given by

$$p_t^P(\cdot) = \eta x_{s,t}^S x_{s,t}^I (S_t x_{s,t}^S + I_t x_{s,t}^I + R_t x_{s,t}^R)^{\alpha-1} I_t. \tag{12}$$

The social planner chooses the paths of home and social activities for each agent by maximizing the weighted sum of the lifetime utilities of all agents. The planner is aware of the dependence of the value function of susceptible individuals on the total share of infected and susceptible individuals. We define the value functions in the planner economy as $\hat{V}_t^i$ for $i \in \{S, I, R\}$. The planner chooses the sequence: $[S_{t+1}, I_{t+1}, R_{t+1}, x_{h,t}^S, x_{h,t}^I, x_{h,t}^R, x_{s,t}^S, x_{s,t}^I, x_{s,t}^R]_{t=0}^{\infty}$ at any initial period t to maximize

$$\hat{V}_t^N = S_t \hat{V}_t^S(S_t, I_t) + I_t \hat{V}_t^I + R_t \hat{V}_t^R \tag{13}$$

with

$$\hat{V}_t^S(S_t, I_t) = U(x_{h,t}^S, x_{s,t}^S) + \beta[p_t^P(\cdot)\hat{V}_{t+1}^I + (1 - p_t^P(\cdot))\hat{V}_{t+1}^S]$$
$$\hat{V}_t^I = U(x_{h,t}^I, x_{s,t}^I) - C^I + \beta[(1-\gamma)\hat{V}_{t+1}^I + \gamma\hat{V}_{t+1}^R]$$
$$\hat{V}_t^R = U(x_{h,t}^R, x_{s,t}^R) + \beta\hat{V}_{t+1}^R$$

and subject to

$$S_{t+1} = S_t - p_t^P(\cdot)S_t$$
$$I_{t+1} = I_t + p_t^P(\cdot)S_t - \gamma I_t$$
$$R_{t+1} = R_t + \gamma I_t,$$

where $S_t + I_t + R_t = N_t \equiv 1 \ \forall t$.

In the social planner's problem, we set $\delta = 0$ since infected agents know that the planner takes into account all the externalities.[12] The first-order conditions for susceptible and infected individuals' home activities and recovered individuals' home and social activities are equivalent to those obtained in the decentralized equilibrium. The social activities of susceptible and infected individuals are instead given by:

$$\frac{\partial U(x_{h,t}^S, x_{s,t}^S)}{\partial x_{s,t}^S} + \beta\frac{\partial p_t^P(\cdot)}{\partial x_{s,t}^S}(\hat{V}_{t+1}^I - \hat{V}_{t+1}^S) + \beta(1 - p_t^P(\cdot))\left(\frac{\partial \hat{V}_{t+1}^S}{\partial S_{t+1}}\frac{\partial S_{t+1}}{\partial x_{s,t}^S} + \frac{\partial \hat{V}_{t+1}^S}{\partial I_{t+1}}\frac{\partial I_{t+1}}{\partial x_{s,t}^S}\right) = 0 \quad (14)$$

$$I_t\frac{\partial U(x_{h,t}^I, x_{s,t}^I)}{\partial x_{s,t}^I} + S_t\left[\beta\frac{\partial p_t^P(\cdot)}{\partial x_{s,t}^I}(\hat{V}_{t+1}^I - \hat{V}_{t+1}^S) + \beta(1 - p_t^P(\cdot))\left(\frac{\partial \hat{V}_{t+1}^S}{\partial S_{t+1}}\frac{\partial S_{t+1}}{\partial x_{s,t}^I} + \frac{\partial \hat{V}_{t+1}^S}{\partial I_{t+1}}\frac{\partial I_{t+1}}{\partial x_{s,t}^I}\right)\right] = 0. \quad (15)$$

Proposition 2. *Suppose $\alpha = 1$. Given the states, the social planner chooses a lower level of social interactions of infected individuals than in the decentralized equilibrium only if the total*

12 All of our results continue to hold, and are in fact reinforced, if $\delta > 0$.

share of susceptible individuals is positive, that is, $S_t > 0$. This holds even for a maximum level of altruism, $\delta = 1$.

Proof. See Appendix A.2.

In our fully dynamic equilibrium model with an infinite horizon, a closed-form analytical solution is not obtainable as the levels of social activity depend on the future value functions. Therefore, to compare the levels of social activity in the social planner's solution and the decentralized equilibrium, we compare the first-order conditions that these levels of social activity solve, and infer the latter's qualitative differences across the two regimes.

We present this comparison in Appendix A.2. The first-order conditions of the planner's problem differ from those of the decentralized economy, and the difference indicates the extent of the externalities that atomistic agents do not internalize in the decentralized equilibrium, which we discuss in the following corollary.

Corollary 3. *The inefficiencies in the decentralized equilibrium can be decomposed into a static inefficiency,*

$$\Phi_t^S = \beta \left[\frac{\partial p_t^P(\cdot)}{\partial x_{s,t}^S} - \frac{p_t(\cdot)}{x_{s,t}^S} \right] (\hat{V}_{t+1}^I - \hat{V}_{t+1}^S) \tag{16}$$

$$\Phi_t^I = \beta \left[\frac{S_t}{I_t} \frac{\partial p_t^P(\cdot)}{\partial x_{s,t}^I} - \delta S_t \frac{p_t}{x_{s,t}^I} \right] (\hat{V}_{t+1}^I - \hat{V}_{t+1}^S), \tag{17}$$

where $\frac{p_t(\cdot)}{x_{s,t}^i} = \frac{\partial p_t(\cdot)}{\partial x_{s,t}^i}$ for $i \in \{S, I\}$, and a dynamic inefficiency,

$$\Psi_t^S = \beta(1 - p_t^P(\cdot)) \left(\frac{\partial \hat{V}_{t+1}^S}{\partial S_{t+1}} \frac{\partial S_{t+1}}{\partial x_{s,t}^S} + \frac{\partial \hat{V}_{t+1}^S}{\partial I_{t+1}} \frac{\partial I_{t+1}}{\partial x_{s,t}^S} \right) \tag{18}$$

$$\Psi_t^I = \beta \frac{S_t}{I_t} (1 - p_t^P(\cdot)) \left(\frac{\partial \hat{V}_{t+1}^S}{\partial S_{t+1}} \frac{\partial S_{t+1}}{\partial x_{s,t}^I} + \frac{\partial \hat{V}_{t+1}^S}{\partial I_{t+1}} \frac{\partial I_{t+1}}{\partial x_{s,t}^I} \right). \tag{19}$$

The static inefficiency is a classical congestion externality due to the fact that atomistic agents do not internalize the impact of their decisions on the average level of social interactions. Its size is affected by the degree of altruism and by the matching function's returns to scale. In

societies with non-altruistic agents or in dense cities, the disease spreads faster in the absence of a central planner, and the size of the inefficiency is larger.

The dynamic inefficiency arises since the planner acts under commitment, and takes into account that the next period's number of susceptible and infected individuals will affect the value function of susceptible individuals through future infection rates. The dynamic inefficiency consists of an *immunity* externality (the first term in the large parentheses) and a *contagion* externality (the second term in the large parentheses), similar to those in Garibaldi et al. (2020a). In principle, these externalities push the optimal level of social activity in opposite directions with the first term being positive and the second one negative. In Appendix A.2 (specifically, in equations (24)-(26)), we show that in our case the contagion externality dominates, leading to a lower level of social activity under the central planner.

Regarding the role of altruism, it follows immediately that:

Corollary 4. *The degree of altruism reduces the size of the static inefficiency.*

Equation (17) reveals that a higher degree of altruism, i.e., a larger δ, reduces the size of the static inefficiency, as it induces infected agents to internalize the cost of their actions on others. However, even a maximum degree of altruism ($\delta = 1$) cannot eliminate the static inefficiency. Importantly, the presence of altruism cannot eliminate the dynamic inefficiency either: the latter depends on the ability to internalize the impact of social interactions on the future evolution of the disease, which is only known to the planner.

SIR-network model. In the SIR-network model, the social planner chooses the sequence $[S^j_{t+1}, I^j_{t+1}, R^j_{t+1}, x^{S,j}_{h,t}, x^{I,j}_{h,t}, x^{R,j}_{h,t}, x^{S,jk}_{s,t}, x^{I,jk}_{s,t}, x^{R,jk}_{s,t}]^{\infty}_{t=0}$ $\forall k$ at any initial period t and for all j to maximize

$$\hat{V}^N_t = \sum_j (S^j_t \hat{V}^{S,j}_t + I^j_t \hat{V}^{I,j}_t + R^j_t \hat{V}^{R,j}_t). \tag{20}$$

The contact probabilities are given by

$$p^{Pj}_t(\cdot) = \sum_k \eta x^{S,jk}_{s,t} x^{I,kj}_{s,t} \frac{m^j \left(\sum_k (x^{S,jk}_{s,t} + x^{I,jk}_{s,t} + x^{R,jk}_{s,t})(\bar{x}^{S,k}_{s,t} S^k_t + \bar{x}^{I,k}_{s,t} I^k_t + \bar{x}^{R,k}_{s,t} R^k_t) \right)}{\sum_k (x^{S,jk}_{s,t} + x^{I,jk}_{s,t} + x^{R,jk}_{s,t})(\bar{x}^{S,k}_{s,t} S^k_t + \bar{x}^{I,k}_{s,t} I^k_t + \bar{x}^{R,k}_{s,t} R^k_t)} I^k_t, \tag{21}$$

with $k = 1, ..., J$ and $\bar{x}_{s,t}^{i,k} = \sum_j x_{s,t}^{i,kj}$ for $i \in \{S, I, R\}$. The first-order conditions for the levels of social activity of susceptible and infected agents in each group j vis-à-vis group k, i.e., $x_{s,t}^{S,jk}$ and $x_{s,t}^{I,jk}$, are reported in Appendix B.

Proposition 3. *Suppose $\alpha = 1$. The social planner chooses a lower level of social interactions of infected individuals of group j vis-à-vis group k than in the decentralized equilibrium only if $\delta I_t^j < N_t^k$, that is, if the number of infected agents in group j multiplied by their level of altruism is smaller than the total population in group k.*

Proof. See Appendix A.3.

Proposition 3 implies that as long as the share of infected agents in group j is smaller than the overall population in group k, the social planner reduces the level of social activity of infected individuals of group j vis-à-vis group k compared to the decentralized equilibrium even if in the latter agents exhibit the maximum level of altruism.

In the SIR-network model, inefficiencies arise as well. Although their types and functional forms are the same as in our baseline model with homogeneous contact rates, their overall size, once aggregated across groups, can vary. The reason for this is that the intensity of social activity across groups depends on heterogeneous, group-specific preferences and risk. For example, altruism can now induce a greater (smaller) reduction of contacts towards more (less) vulnerable groups.

Policy implementation. The presence of inefficiencies can be addressed by means of a policy implementation. We focus on the role of general lockdown policies, a prominent class of non-pharmaceutical interventions during the COVID-19 pandemic.

The planner is endowed with one instrument, namely the mandatory restriction of social activity of susceptible, infected, and recovered agents. We denote by θ the fraction of mandatory restricted social activity. We show under what conditions the stringency policy θ can achieve efficiency, equalizing the ratio of the marginal utility from social activity for an infected agent and the one for a susceptible agent, which we henceforth refer to as the marginal rate of substitution between one infected and one susceptible agent, in the

decentralized (DE) and the social planner's (SP) equilibrium. For simplicity, we focus on the homogeneous model with a maximum degree of altruism, $\delta = 1$.[13] In the SIR-network model, the same implementation result would hold, albeit targeted at each individual group.

Proposition 4. *The marginal rates of substitution between one infected and one susceptible agent in the decentralized and in the social planner's equilibrium become equivalent if the planner sets a stringency measure θ so as to equalize the infection probabilities across the two equilibria, that is:*

$$p_t(\theta, \cdot) = \eta(1-\theta)x^S_{s,t}(1-\theta)x^I_{s,t}\frac{m((1-\theta)\bar{x}_{s,t})}{(1-\theta)\bar{x}_{s,t}}I_t. \tag{22}$$

Proof. See Appendix A.4.

If the infection probabilities are equal in the two equilibria, the static inefficiency is eliminated under full altruism, $\delta = 1$. Beyond that, if the social planner's infection probabilities are enforced under the decentralized equilibrium, the dynamic inefficiency is eliminated as well, as the dynamic of the pandemic follows the one in the social planner's solution.

3. Quantitative Analysis

In this section, we simulate the two variants of our model. The first goal is to ascertain the impact of social-activity choices on the dynamics of infections by comparing our baseline SIR model with optimizing agents to the traditional version with exogenous contact rates. Furthermore, we demonstrate the importance of altruism in shaping agents' behavior and flattening the infection curve, and confirm our analytical findings for both the homogeneous and the SIR-network model. Finally, we illustrate the solutions under a central planner and quantify the role of optimal lockdown policies implemented by a Ramsey planner, who takes as given the optimizing conditions of agents.

13 Note that if $\delta < 1$, the marginal rates of substitution become equivalent up to a factor of $\frac{1}{\delta}$, i.e., $MRS^{DE}_{t,I,S} = \frac{1}{\delta}MRS^{SP}_{t,I,S}$.

3.1. Calibration

The instantaneous utility of susceptible and infected individuals is a function of their social activities $x^S_{s,t}$ and $x^I_{s,t}$, respectively.[14] The functional forms read as follows: $U(x^S_{s,t}) = c_S \log(x^S_{s,t}) - x^S_{s,t} + 1$ and $U(x^I_{s,t}) = c_I \log(x^I_{s,t}) - x^I_{s,t} + 1$ for susceptible and infected individuals. c_S and c_I denote the respective steady-state levels of social activity, and could in principle differ from each other since infected agents may go out less because they do not feel well. However, for simplicity we set both equal to 1, implying a steady-state level of social activity of 1 and a maximum utility of 0.

Infected individuals pay an infection cost C_I while being infected. The calibration of this cost is based on the infection fatality rate and the value of a statistical life (VSL), as suggested by Hall et al. (2020). We follow Farboodi et al. (2021) and set the former to 0.0062, which is the intermediate infection probability of two baseline scenarios in Hall et al. (2020). The VSL is calculated from Hall et al. (2020)'s estimate of the value of each remaining year of life, \$270,000, and the average remaining life expectancy of COVID-19 victims of 14.5 years, translated to the model units.[15] In general, the infection cost C_I might depend on the congestion of the health system, which in turn depends on the number of infected individuals. We abstract from this dependence but note that its inclusion would strengthen our conclusions: susceptible and altruistic infected agents aware of the health-system congestion would reduce their social activity even more when the number of infections is high.

We set $\alpha = 1$, implying a quadratic matching function. The recovery rate γ is 1/10. The implied infection duration of 10 days matches different quarantine rules applied in reality and considered in other papers simulating the COVID-19 pandemic.[16] In the SIR-network model, we will consider three age groups that differ in their recovery rates. As in Acemoglu et al. (2021), the three groups are the young ($20-49$ years), middle-aged ($50-64$ years), and old (65+ years) with respective population shares of $N_y = 53\%$, $N_m = 26\%$, and $N_o = 21\%$. We

14 We assume that in steady state the utility functions of recovered and susceptible individuals are the same. Recovered individuals do not modify their social activity since they become immune. Furthermore, we do not analyze home activities here since they do not influence our results.

15 A more detailed description of the calculations can be found in Farboodi et al. (2021). To map the VSL to the model units, one first computes the fraction of consumption an individual would be willing to pay to avoid a certain death risk and then calculates which VSL would solve the equivalent utility loss.

16 For example, Farboodi et al. (2021) choose a recovery rate of 1/7 and Dasaratha (2022) a rate of 1/14.

Table 1
Calibration

Parameter	Value	Description
α	1	Matching function's returns to scale
$c_S = c_I$	1	Steady-state social activity
γ	1/10	Recovery rate
η	2.5*γ	Transmission rate
C_I	197	Cost of infection
δ	[0,1]	Degree of altruism
β	0.99	Discount factor
ϵ	0.0001	Initial infection shock of 0.01%
γ_y	1/7	Recovery rate young
γ_m	1/10	Recovery rate middle-aged
γ_o	1/14	Recovery rate old
N_y	0.53	Population share young
N_m	0.26	Population share middle-aged
N_o	0.21	Population share old

choose the recovery rates such that the young agents recover faster and the old ones do so more slowly than in the homogeneous version of our model. Specifically, we set $\gamma_y = 1/7$, $\gamma_m = 1/10$, and $\gamma_o = 1/14$. The disease transmission rate η is chosen so as to match a basic reproduction number $R_0 = \frac{\eta}{\gamma}$ of 2.5, which is Burki (2021)'s estimate for the original strain of SARS-CoV-2. The degree of altruism δ is between 0 and 1, and set to 0.5 in our baseline simulations. The discount factor β is set to 0.99. Table 1 provides an overview of the parameter values.

For the simulations, we assume that initially the economy is in a steady state with no infections and then hit by a zero-probability MIT shock, increasing the total share of infected agents from 0 to ϵ. ϵ is set to $0.0001 = 0.01\%$, as in, e.g., Brotherhood et al. (2020). Details on the computations and the model equations are given in Appendix D.

3.2. Simulation Results

We now discuss the simulation results based on our calibration, with the goal of quantifying the role of altruism, the extent of externalities, and how altruism may affect the latter.

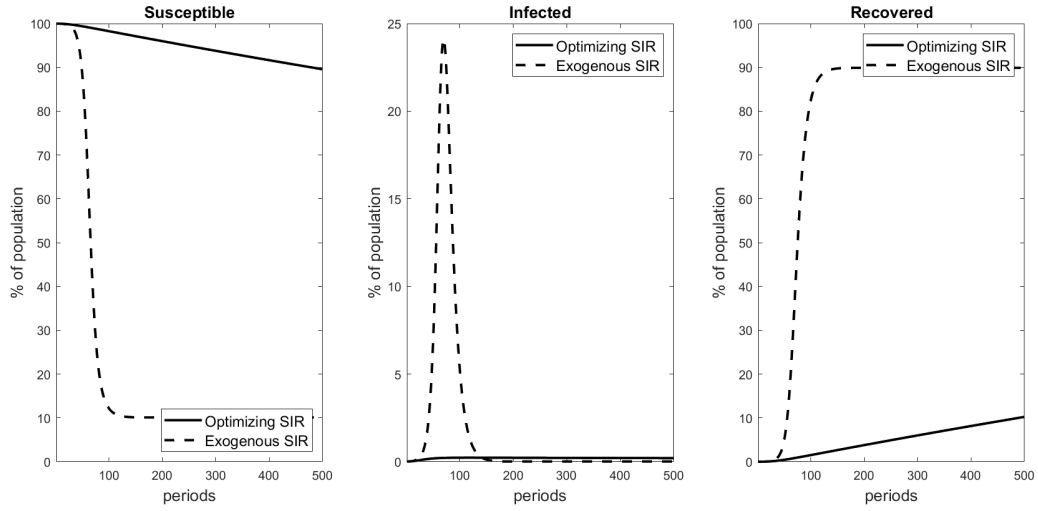

Figure 1
Comparison of the Homogeneous SIR Model with Endogenous Social Activity ($\delta = 0.5$) and the Traditional SIR Model with Constant Exogenous Contact Rates

Homogeneous optimizing SIR model with different degrees of altruism vs. traditional SIR model. Figure 1 compares the dynamics of the total shares of susceptible, infected, and recovered individuals in our homogeneous SIR model with endogenous social activity with the ones in the traditional SIR model with exogenous contact rates. For this purpose, in the latter social activity is set to a constant value equal to the average steady-state level of social activity, i.e., 1. The other parameters are the same across the two models.

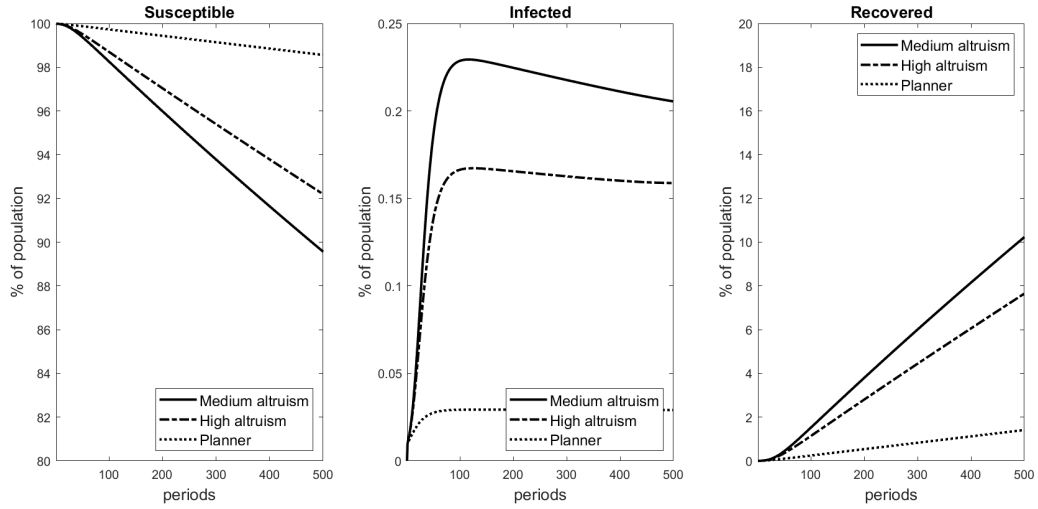

Figure 2
Comparison of the Decentralized Equilibrium with Different Degrees of Altruism and the Social Planner's Solution

First, Figure 1 shows that the peak of the infection curve (middle panel) is significantly

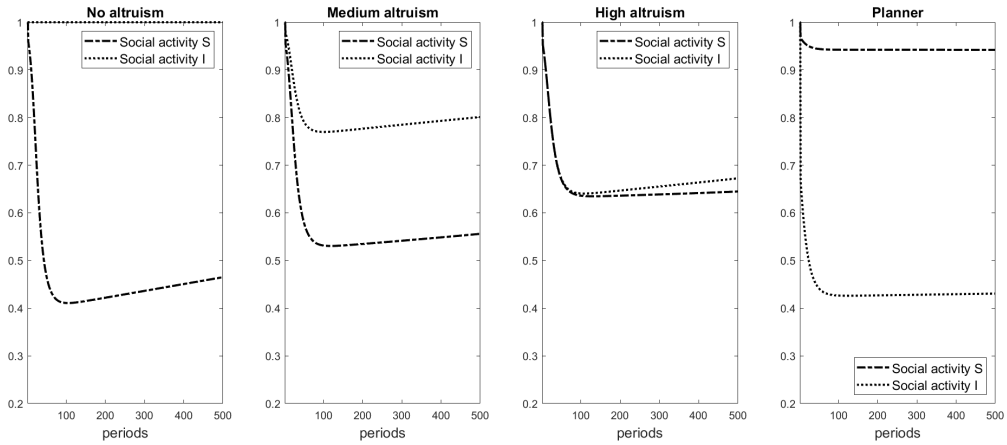

Figure 3
Comparison of Social Activity of Susceptible (S) and Infected (I) Individuals in the Decentralized Equilibrium with Different Degrees of Altruism and the Social Planner's Solution

flattened in the model with endogenous social activity. This illustrates the fundamental role of behavioral responses to infection risk in determining the dynamic of a pandemic. As susceptible agents internalize the consequences of this risk for their future utility, they become more cautious and reduce their level of social activity. This holds in general for any degree of altruism of infected individuals, and in the absence of any lockdown. Due to this more careful behavior, the infection probability in the optimizing SIR model drops, which explains why the share of susceptible individuals remains higher than under exogenous contact rates. This significant difference bears relevance, for example, for planning the availability of sufficient healthcare units.

Figure 2 demonstrates the role of altruism in flattening the curve further by reducing the total share of infected individuals. We set δ to 0.5 and 1, representing medium and high degrees of altruism, respectively. The more altruistic infected individuals are the more they reduce their social activity, lowering the infection probability which, in turn, leads to a lower share of infected individuals.

The different levels of social activity depending on the degree of altruism are displayed in Figure 3. When infected individuals are not altruistic at all (left panel), they do not alter their behavior in response to the pandemic. However, when they exhibit a high—in fact, maximum—degree of altruism ($\delta = 1$, second rightmost panel), they reduce their

social activity on impact in response to the infection shock by roughly the same amount as susceptible individuals do.[17] Consistent with Proposition 1, Figure 3 shows as well that when the degree of altruism increases, susceptible individuals reduce their social contacts by less since infected individuals carry part of the burden by internalizing some of the infection risk.

Social planner vs. decentralized equilibrium. Our results may lead one to believe that a society with the maximum degree of altruism may not need any planning intervention. This is, however, not the case. As can be seen in Figure 2 (two leftmost panels), the number of infected individuals is lower but the number of susceptible individuals is higher in the social planner's solution than in the decentralized solution with the maximum degree of altruism ($\delta = 1$). As the rightmost panel of Figure 3 shows, this is consistent with the fact that the social planner reduces the level of social activity of infected individuals significantly more in comparison to the decentralized equilibrium, illustrating Proposition 2. This, in turn, allows susceptible agents to reduce their social contacts by less compared to the decentralized equilibrium.

To explain why this is the case, we consider the two types of inefficiencies described in Corollary 3. First, the presence of altruism reduces the extent of the static inefficiency, but only up to the degree of congestion given by the geography, i.e., the returns to scale of the matching function. Second, and more importantly, altruism does not reduce the extent of the dynamic inefficiency. The existence of a dynamic inefficiency constitutes a crucial difference in comparison to other models. Farboodi et al. (2021), for instance, briefly discuss the consequences of adding altruism in the form of a weight on the current utility of susceptible individuals. In their model, the social planner's solution coincides with the fully altruistic equilibrium. In our model, this is not the case due to dynamic considerations. The planner internalizes the risk of infection not only at time t but also in all future periods (as highlighted in a different context also by Moser and Yared, 2022).

SIR-network model with endogenous choice of group-differentiated social activity.

17 Note that as the pandemic progresses, the social activity of infected individuals exceeds that of susceptible individuals, as the former take into account the population share of susceptible individuals, which is decreasing over time.

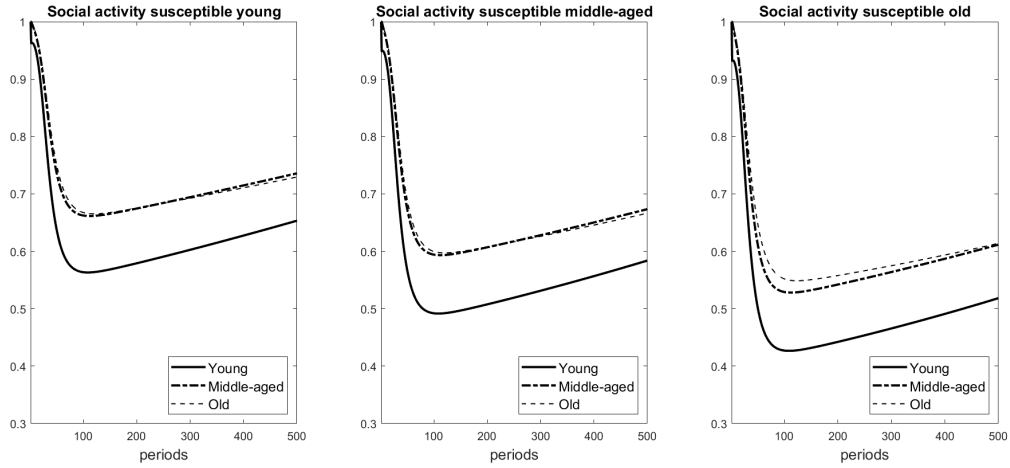

Figure 4
Differentiated Social Activity of Susceptible Young, Middle-aged, and Old Individuals in the SIR-Network Model ($\delta = 0.5$)

We now simulate the model in which agents of different groups interact with one another. These groups differ in terms of their recovery rates.[18] In what follows, we will interpret the three groups with different recovery rates as three different age groups. We assume that the infection shock occurs in the group of young agents. In this version of the model, the social intensity of agents of each group vis-à-vis each other group is chosen endogenously. For the following simulations, we choose a medium degree of altruism ($\delta = 0.5$).

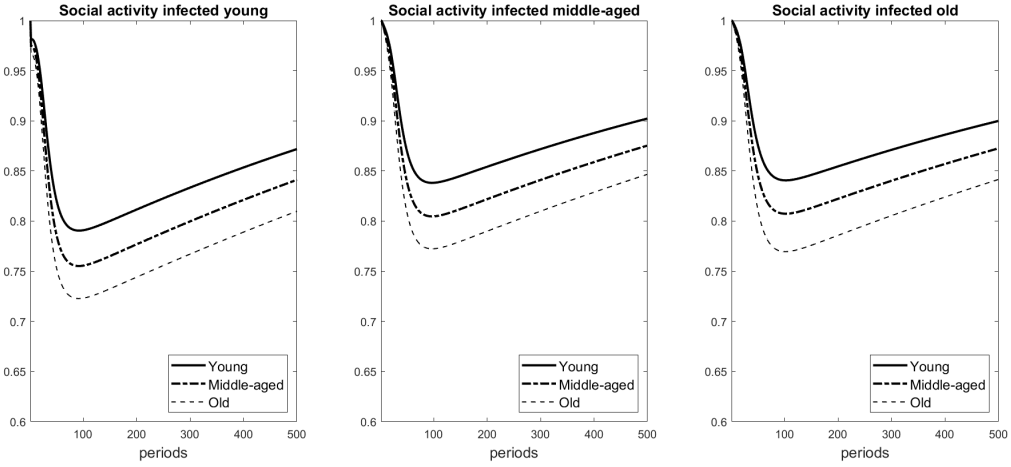

Figure 5
Differentiated Social Activity of Infected Young, Middle-aged, and Old Individuals in the SIR-Network Model ($\delta = 0.5$)

Figure 4 shows the social-activity intensities of susceptible young, middle-aged, and old agents vis-à-vis the three different groups relative to their steady-state levels. Susceptible

18 Note that setting different infection costs across groups would not affect our results.

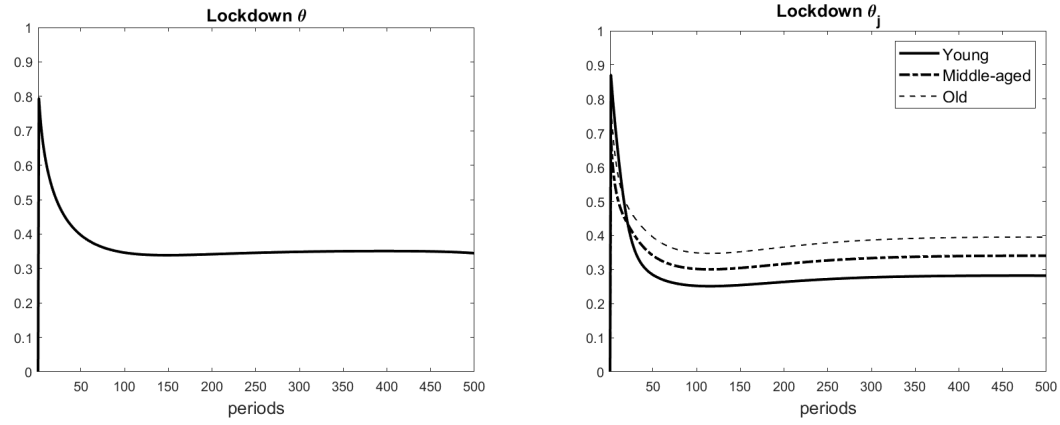

(a) Homogeneous model **(b) Network model**

Figure 6
Optimal Lockdown in the Homogeneous SIR and the SIR-Network Model ($\delta = 0.5$)

old agents reduce their overall social activity the most due to their lower recovery rates. Susceptible young agents, in turn, reduce their social activity the least and have, therefore, the highest infection probability, as Figure 8 in Appendix C shows. In terms of differentiated social activity, reflecting Corollary 1, all three groups primarily reduce their contact exposure to young agents (solid line), as the latter are in the group with the highest share of infected agents and therefore the most significant spreaders.[19] Figure 5 illustrates Corollary 2: even for a medium degree of altruism, infected agents reduce their social activity the most vis-à-vis the most vulnerable group with the lowest recovery rate, namely the old agents.

Figure 9 in Appendix C presents the aggregate levels of social-activity intensity of all three susceptible age groups for two different degrees of altruism ($\delta = 0.5$ vs. 1). All—and especially old—susceptible agents reduce their social activity by less when infected individuals are more altruistic (see left vs. right panel). This is again driven by the fact that—especially young—infected agents that are more altruistic reduce their activity by more as a higher degree of altruism makes them more cautious, as Figure 10 in Appendix C showcases.

Optimal lockdown policy in the homogeneous SIR and the SIR-network model. We conclude our analysis by quantifying the optimal lockdown policy for both the homogeneous (baseline) SIR and the SIR-network model. Figure 6 plots the optimal lockdown policy as captured by the fraction θ of social activity chosen by a Ramsey planner in the homogeneous

19 Figure 7 in Appendix C displays the course of the pandemic separately for the three age groups with endogenous vs. exogenous contact rates.

SIR model (left panel) and the SIR-network model (right panel). All remaining parameters are as before, with a medium degree of altruism ($\delta = 0.5$). The Ramsey planner sets a very strict lockdown at the beginning of the pandemic so as to cut the share of infected agents immediately to a bearable level, and then relaxes stringency measures accordingly.

In the SIR-network model, lockdown policies are set differentially across age groups. On impact, the planner optimally restricts social interactions in the young age group the most, as these are the agents with the highest infection numbers. After this immediate reaction, lockdowns are strictest for the old age group since the disease is most dangerous for its members. While a complete lockdown of a single group (i.e., sequestering) while granting full freedom for all other groups would be unethical, joint burden-sharing with differential protective non-pharmaceutical interventions across groups would be desirable in light of the different recovery rates across groups. A practical implementation of this policy would comprise, for example, more extensive leaves of absence for older workers or other groups with pre-existing health conditions.

4. Conclusion

Understanding the determinants of behavioral responses in the face of catastrophic events, such as a pandemic, is important along at least two dimensions. First, it is difficult to accurately forecast the spread of a disease with models that do not account for human behavior. Second, as policymakers deliberate on optimal stringency policies to mitigate the loss of lives and adverse economic consequences, incorporating individuals' heterogeneous behavior is visceral even as lockdowns and other stringency measures are lifted.

In our model with endogenous contact rates, agents internalize the consequences of the infection risk, become more cautious, and reduce their level of social activity voluntarily. We uncover important sources of heterogeneity in individuals' behavior, in particular a significant role for altruism, which we demonstrate in a homogeneous SIR and an SIR-network model. By affecting both infected and susceptible individuals' behavior, altruism can contribute to flattening the infection curve. However, we show that even in the presence of a maximum

degree of altruism, non-negligible health externalities remain. To address them, a social planner would choose a sharp lockdown for all on impact before restricting social activities primarily for vulnerable groups. Our model can be easily extended to include other dimensions of heterogeneity, add uncertainty, or study different policy interventions, which we leave for future research.

References

Acemoglu, D., Chernozhukov, V., Werning, I., and Whinston, M. D. (2021). Optimal Targeted Lockdowns in a Multigroup SIR Model. *American Economic Review: Insights*, 3(4):487–502.

Alfaro, L., Faia, E., Lamersdorf, N., and Saidi, F. (2022). Health Externalities and Policy: The Role of Social Preferences. *Management Science*, 68(9):6355–7064.

Ambrus, A., Mobius, M., and Szeidl, A. (2014). Consumption Risk-Sharing in Social Networks. *American Economic Review*, 104(1):149–182.

Andreoni, J. (1989). Giving with Impure Altruism: Applications to Charity and Ricardian Equivalence. *Journal of Political Economy*, 97(6):1447–1458.

Andreoni, J. (1993). An Experimental Test of the Public-Goods Crowding-Out Hypothesis. *American Economic Review*, 83(5):1317–1327.

Andreoni, J. and Miller, J. (2002). Giving according to GARP: An Experimental Test of the Consistency of Preferences for Altruism. *Econometrica*, 70(2):737–753.

Becker, G. S. (1974). A Theory of Social Interactions. *Journal of Political Economy*, 82(6):1063–1093.

Becker, G. S. (1996). Preferences and Values. In *Accounting for Tastes*, pages 1–23. Harvard University Press.

Bloch, F., Génicot, G., and Ray, D. (2008). Informal Insurance in Social Networks. *Journal of Economic Theory*, 143(1):36–58.

Bolton, G. E. and Ockenfels, A. (2000). ERC: A Theory of Equity, Reciprocity, and Competition. *American Economic Review*, 90(1):166–193.

Bramoullé, Y. and Kranton, R. (2007). Risk-Sharing Networks. *Journal of Economic Behavior & Organization*, 64(3-4):275–294.

Brock, W. A. and Durlauf, S. N. (2001). Discrete Choice with Social Interactions. *Review of Economic Studies*, 68(2):235–260.

Brotherhood, L., Kircher, P., Santos, C., and Tertilt, M. (2020). An Economic Model of the Covid-19 Pandemic with Young and Old Agents: Behavior, Testing and Policies. *CEPR Discussion Paper No. 14695*.

Burki, T. K. (2021). Omicron Variant and Booster COVID-19 Vaccines. *The Lancet Respiratory Medicine*, 10(2).

Cabrales, A., Calvó-Armengol, A., and Zenou, Y. (2011). Social Interactions and Spillovers. *Games and Economic Behavior*, 72(2):339–360.

Case, A. C. and Katz, L. F. (1991). The Company You Keep: The Effects of Family and Neighborhood on Disadvantaged Youths. *NBER Working Paper No. 3705*.

Casoria, F., Galeotti, F., and Villeval, M. C. (2021). Perceived Social Norm and Behavior Quickly Adjusted to Legal Changes during the COVID-19 Pandemic. *Journal of Economic Behavior & Organization*, 190:54–65.

Casoria, F., Galeotti, F., and Villeval, M. C. (2023). Trust and Social Preferences in Times of Acute Health Crisis. *IZA Discussion Paper No. 15929*.

Chakrabarti, S., Krasikov, I., and Lamba, R. (2022). Behavioral Epidemiology: An Economic Model to Evaluate Optimal Policy in the Midst of a Pandemic. *Penn State University Working Paper*.

Currarini, S., Jackson, M. O., and Pin, P. (2009). An Economic Model of Friendship: Homophily, Minorities, and Segregation. *Econometrica*, 77(4):1003–1045.

Dasaratha, K. (2022). Virus Dynamics with Behavioral Responses. *Yale University Working Paper*.

Diamond, P. A. (1982). Aggregate Demand Management in Search Equilibrium. *Journal of Political Economy*, 90(5):881–894.

Doepke, M. and Tertilt, M. (2009). Women's Liberation: What's in It for Men? *Quarterly Journal of Economics*, 124(4):1541–1591.

Duffie, D., Gârleanu, N., and Pedersen, L. H. (2005). Over-the-Counter Markets. *Econometrica*, 73(6):1815–1847.

Falk, A., Becker, A., Dohmen, T., Enke, B., Huffman, D., and Sunde, U. (2018). Global Evidence on Economic Preferences. *Quarterly Journal of Economics*, 133(4):1645–1692.

Farboodi, M., Jarosch, G., and Shimer, R. (2021). Internal and External Effects of Social Distancing in a Pandemic. *Journal of Economic Theory*, 196:105293.

Farboodi, M., Jarosch, G., and Shimer, R. (2023). The Emergence of Market Structure. *Review of Economic Studies*, 90(1):261–292.

Fehr, E. and Gächter, S. (2000). Fairness and Retaliation: The Economics of Reciprocity. *Journal of Economic Perspectives*, 14(3):159–181.

Fehr, E. and Schmidt, K. M. (1999). A Theory of Fairness, Competition, and Cooperation. *Quarterly Journal of Economics*, 114(3):817–868.

Fortin, B., Lacroix, G., and Villeval, M. C. (2007). Tax Evasion and Social Interactions. *Journal of Public Economics*, 91(11-12):2089–2112.

Frey, B. S. and Meier, S. (2004). Pro-social Behavior in a Natural Setting. *Journal of Economic Behavior & Organization*, 54(1):65–88.

Garibaldi, P., Moen, E. R., and Pissarides, C. A. (2020a). Modelling Contacts and Transitions in the SIR Epidemics Model. *Covid Economics: Vetted and Real-Time Papers*, 5.

Garibaldi, P., Moen, E. R., and Pissarides, C. A. (2020b). Static and Dynamic Inefficiencies in an Optimizing Model of Epidemics. *CEPR Discussion Paper No. 15439*.

Glaeser, E. L., Sacerdote, B., and Scheinkman, J. A. (1996). Crime and Social Interactions. *Quarterly Journal of Economics*, 111(2):507–548.

Gollier, C. (2020). Cost–benefit Analysis of Age-specific Deconfinement Strategies. *Journal of Public Economic Theory*, 22(6):1746–1771.

Hall, R. E., Jones, C. I., and Klenow, P. J. (2020). Trading off Consumption and COVID-19 Deaths. *Minneapolis Fed Quarterly Review*, 42(1).

Hethcote, H. W. (2000). The Mathematics of Infectious Diseases. *SIAM Review*, 42(4):599–653.

Hofstede, G. (2001). *Culture's Consequences: Comparing Values, Behaviors, Institutions and Organizations across Nations*. Sage Publications.

Kermack, W. O. and McKendrick, A. G. (1927). A Contribution to the Mathematical Theory of Epidemics. *Proceedings of the Royal Society of London*, 115(772):700–721.

Kremer, M. (1996). Integrating Behavioral Choice into Epidemiological Models of AIDS. *Quarterly Journal of Economics*, 111(2):549–573.

Moinet, A., Pastor-Satorras, R., and Barrat, A. (2018). Effect of Risk Perception on Epidemic Spreading in Temporal Networks. *Physical Review E*, 97:012313.

Moser, C. and Yared, P. (2022). Pandemic Lockdown: The Role of Government Commitment. *Review of Economic Dynamics*, 46:27–50.

Pastor-Satorras, R. and Vespignani, A. (2001a). Epidemic Dynamics and Endemic States in Complex Networks. *Physical Review E*, 63(6):066117.

Pastor-Satorras, R. and Vespignani, A. (2001b). Epidemic Spreading in Scale-Free Networks. *Physical Review Letters*, 86(14):3200–3203.

Perra, N., Gonçalves, B., Pastor-Satorras, R., and Vespignani, A. (2012). Activity Driven Modeling of Time Varying Networks. *Scientific Reports*, 2(469).

Petrongolo, B. and Pissarides, C. A. (2001). Looking into the Black Box: A Survey of the Matching Function. *Journal of Economic Literature*, 39(2):390–431.

Pissarides, C. A. (2000). *Equilibrium Unemployment Theory*. The MIT Press, 2nd edition.

Rubinstein, A. and Wolinsky, A. (1987). Middlemen. *Quarterly Journal of Economics*, 102(3):581–593.

Spolaore, E. and Wacziarg, R. (2013). How Deep are the Roots of Economic Development? *Journal of Economic Literature*, 51(2):325–369.

Wu, L. and Shimer, R. (2021). Diffusion on a Sorted Network. *University of Chicago Working Paper*.

A. Proofs

A.1. Proof of Proposition 1

The first-order condition for infected individuals who exhibit a non-zero degree of altruism is $\frac{\partial U(x^I_{h,t},x^I_{s,t})}{\partial x^I_{s,t}} + \delta S_t \beta \frac{\partial p_t(\cdot)}{\partial x^I_{s,t}}(V^I_{t+1} - V^S_{t+1}) = 0$. If they do not exhibit any altruism, i.e., $\delta = 0$, it becomes $\frac{\partial U(x^I_{h,t},x^I_{s,t})}{\partial x^I_{s,t}} = 0$. Since $V^I_{t+1} - V^S_{t+1} < 0$, the term $\frac{\partial U(x^I_{h,t},x^I_{s,t})}{\partial x^I_{s,t}}$ has to be larger in the presence of altruism ($\delta > 0$) and, thus, the $x^I_{s,t}$ that solves the first equation with altruism is smaller. The larger the degree of altruism δ, the larger the marginal utility, $\frac{\partial U(x^I_{h,t},x^I_{s,t})}{\partial x^I_{s,t}}$, and, thus, the smaller $x^I_{s,t}$.

From the first-order condition for the susceptible individuals, (8), it follows that $\frac{\partial U(x^S_{h,t},x^S_{s,t})}{\partial x^S_{s,t}} = \beta \frac{\partial p_t(\cdot)}{\partial x^S_{s,t}}(V^S_{t+1} - V^I_{t+1}) = \beta \eta x^I_{s,t}(\overline{x}_{s,t})^{\alpha-1} I_t (V^S_{t+1} - V^I_{t+1})$. Given the states, if $x^I_{s,t}$ is lower when infected individuals exhibit altruism, it follows that $\frac{\partial U(x^S_{h,t},x^S_{s,t})}{\partial x^S_{s,t}}$ is lower as well, implying a larger $x^S_{s,t}$. The lower $x^I_{s,t}$, the lower $\frac{\partial U(x^S_{h,t},x^S_{s,t})}{\partial x^S_{s,t}}$ and, thus, the larger $x^S_{s,t}$.

A.2. Proof of Proposition 2

We compare the first-order conditions for social activities of infected individuals in the decentralized and the social planner's equilibrium, namely (9) and (15).[20] To prove that the social activity of infected agents chosen by the social planner is lower than in the decentralized equilibrium, we show that

$$\beta \left[\frac{S_t}{I_t} \frac{\partial p^P_t(\cdot)}{\partial x^I_{s,t}} - \delta S_t \frac{\partial p_t}{\partial x^I_{s,t}} \right] (\hat{V}^I_{t+1} - \hat{V}^S_{t+1}) + \beta \frac{S_t}{I_t}(1 - p^P_t(\cdot)) \left(\frac{\partial \hat{V}^S_{t+1}}{\partial S_{t+1}} \frac{\partial S_{t+1}}{\partial x^I_{s,t}} + \frac{\partial \hat{V}^S_{t+1}}{\partial I_{t+1}} \frac{\partial I_{t+1}}{\partial x^I_{s,t}} \right) < 0, \tag{23}$$

where $p^P_t(\cdot)$ is given by (12). Only if the inequality in (23) holds, the social planner chooses a higher marginal utility and, hence, a lower level of social activity of infected individuals.

20 Note that we compare the decentralized equilibrium with any degree of altruism to the social planner's equilibrium without altruism. We set $\delta = 0$ in the latter since in the presence of a central social planner, infected agents know that the planner takes into account all the externalities, which is why there is no particular role for altruism in that instance. However, one can show that our results would continue to hold if $\delta > 0$ also in the social planner's equilibrium.

We first examine the second term of (23). Note that:

$$\frac{\partial \hat{V}^S_{t+1}}{\partial S_{t+1}}\frac{\partial S_{t+1}}{\partial x^I_{s,t}} + \frac{\partial \hat{V}^S_{t+1}}{\partial I_{t+1}}\frac{\partial I_{t+1}}{\partial x^I_{s,t}} = \left(-\frac{\partial \hat{V}^S_{t+1}}{\partial S_{t+1}} + \frac{\partial \hat{V}^S_{t+1}}{\partial I_{t+1}}\right)\frac{\partial p^P_t(\cdot)}{\partial x^I_{s,t}} S_t \tag{24}$$

$$= \beta(\hat{V}^I_{t+2} - \hat{V}^S_{t+2})\left[-\frac{\partial p^P_{t+1}(\cdot)}{\partial S_{t+1}} + \frac{\partial p^P_{t+1}(\cdot)}{\partial I_{t+1}}\right]\frac{\partial p^P_t(\cdot)}{\partial x^I_{s,t}} S_t. \tag{25}$$

Note further that:

$$\begin{aligned}-\frac{\partial p^P_{t+1}(\cdot)}{\partial S_{t+1}} + \frac{\partial p^P_{t+1}(\cdot)}{\partial I_{t+1}} =& -(\alpha-1)\eta x^S_{s,t+1}x^I_{s,t+1}(\overline{x}_{s,t+1})^{\alpha-2} I_{t+1}x^S_{s,t+1} + \\ &+ (\alpha-1)\eta x^S_{s,t+1}x^I_{s,t+1}(\overline{x}_{s,t+1})^{\alpha-2} I_{t+1}x^I_{s,t+1} + \eta x^S_{s,t+1}x^I_{s,t+1}(\overline{x}_{s,t+1})^{\alpha-1}.\end{aligned} \tag{26}$$

Under $\alpha = 1$, implying a quadratic matching function, this last expression, (26), is positive.[21] Therefore, the second term in (23) is negative only if $\hat{V}^I_{t+2} - \hat{V}^S_{t+2} < 0$ (Assumption 1) and $S_t > 0$, since $\frac{\partial p^P_t(\cdot)}{\partial x^I_{s,t}} > 0$ and $p^P_t(\cdot) < 1$.

The first part of (23) is negative as well only if $\hat{V}^I_{t+1} - \hat{V}^S_{t+1} < 0$ and $\frac{S_t}{I_t}\frac{\partial p^P_t(\cdot)}{\partial x^I_{s,t}} > \delta S_t \frac{\partial p_t}{\partial x^I_{s,t}}$. With $\alpha = 1$, we can write the latter condition as: $\frac{S_t}{I_t}\eta x^S_{s,t} I_t > \delta S_t \eta x^S_{s,t} I_t$. The inequality holds for any δ, only if the share of susceptible agents is positive, $S_t > 0$, implying $I_t < 1$.

To sum up, only if the whole expression in (23) is negative, the marginal utility of social interactions of infected individuals chosen by the social planner is larger than the one under the decentralized equilibrium, which means that the level of social activities of infected individuals, $x^I_{s,t}$, chosen by the social planner is smaller.

A.3. Proof of Proposition 3

To compare the solutions of the decentralized and the social planner's equilibrium in the endogenous network variant of our model, we again compare the first-order conditions for social activities of infected individuals of group j vis-à-vis group k, $x^{I,jk}_{s,t}$, namely (11) and

21 It would also be positive for different values of α if the total share of infected agents, I_{t+1}, is close to zero.

(34). As before, the social planner chooses a lower level for the social activity of infected individuals in group j vis-à-vis group k only if

$$\frac{1}{I_t^j}\sum_n S_t^n \beta \frac{\partial p_t^{Pn}(\cdot)}{\partial x_{s,t}^{I,jk}}(\hat{V}_{t+1}^{I,n} - \hat{V}_{t+1}^{S,n}) - \delta \frac{S_t^k}{N_t^k}\beta \frac{\partial p_t^k(\cdot)}{\partial x_{s,t}^{I,jk}}(V_{t+1}^{I,k} - V_{t+1}^{S,k})$$
$$+\frac{1}{I_t^j}\sum_n S_t^n \beta (1 - p_t^{Pn}(\cdot)) \sum_m \left(\frac{\partial \hat{V}_{t+1}^{S,n}}{\partial S_{t+1}^m}\frac{\partial S_{t+1}^m}{\partial x_{s,t}^{I,jk}} + \frac{\partial \hat{V}_{t+1}^{S,n}}{\partial I_{t+1}^m}\frac{\partial I_{t+1}^m}{\partial x_{s,t}^{I,jk}} \right) < 0, \tag{27}$$

where p_t^{Pn} is given by equation (21) and (the summations over) n and m refer to all groups, including j and k.

We proceed as in the proof for Proposition 2 and argue that only if the inequality (27) holds, the social planner chooses a higher marginal utility and, hence, a lower level of social activity. As before, under the assumption of a quadratic matching function, i.e., $\alpha = 1$, the last term on the left-hand side of (27) is negative for all groups n only if $\hat{V}_{t+2}^{I,n} - \hat{V}_{t+2}^{S,n} < 0$.

To show that the remaining expression is negative as well, we show that $\frac{1}{I_t^j}\sum_n S_t^n \beta \frac{\partial p_t^{Pn}(\cdot)}{\partial x_{s,t}^{I,jk}}(\hat{V}_{t+1}^{I,n} - \hat{V}_{t+1}^{S,n}) - \delta \frac{S_t^k}{N_t^k}\beta \frac{\partial p_t^k(\cdot)}{\partial x_{s,t}^{I,jk}}(V_{t+1}^{I,k} - V_{t+1}^{S,k}) < 0$. Due to our assumptions for the matching function and $\alpha = 1$, this becomes $\beta \left[\frac{1}{I_t^j} S_t^k \frac{\partial p_t^{Pk}(\cdot)}{\partial x_{s,t}^{I,jk}} - \delta \frac{S_t^k}{N_t^k}\frac{\partial p_t^k(\cdot)}{\partial x_{s,t}^{I,jk}} \right](\hat{V}_{t+1}^{I,k} - \hat{V}_{t+1}^{S,k}) < 0$. According to Assumption 1, $(V_{t+1}^{I,k} - V_{t+1}^{S,k}) < 0$, therefore, this inequality holds only if $\frac{S_t^k}{I_t^j}\eta x_{s,t}^{S,kj} I_t^j > \delta \frac{S_t^k}{N_t^k}\eta x_{s,t}^{S,kj} I_t^j$, which is the case if $\delta I_t^j < N_t^k$. Hence, if the number of infected agents in group j multiplied by their level of altruism is smaller than the total population in group k, the social planner reduces the level of social activity of infected agents of group j vis-à-vis group k by more compared to the decentralized equilibrium.

A.4. Proof of Proposition 4

We start by obtaining the ratio of the marginal utility from the social activity for an infected agent and the marginal utility from the social activity for a susceptible agent, which we dub

the marginal rate of substitution between one infected and one susceptible agent, in the decentralized economy (DE) at time t (in the case with maximum altruism, $\delta = 1$):

$$MRS^{DE}_{t,I,S} = \frac{\frac{\partial U(x^I_{h,t}, x^I_{s,t})}{\partial x^I_{s,t}}}{\frac{\partial U(x^S_{h,t}, x^S_{s,t})}{\partial x^S_{s,t}}} = \frac{\frac{\partial p_t}{\partial x^I_{s,t}}}{\frac{\partial p_t}{\partial x^S_{s,t}}}. \tag{28}$$

The respective marginal rate of substitution in the social planner's (SP) solution is:

$$MRS^{SP}_{t,I,S} = \frac{\frac{\partial p^P_t}{\partial x^I_{s,t}}(V^I_{t+1} - V^S_{t+1}) + (1 - p^P_t)\Psi^I_t}{\frac{\partial p^P_t}{\partial x^S_{s,t}}(V^I_{t+1} - V^S_{t+1}) + (1 - p^P_t)\Psi^S_t}, \tag{29}$$

where

$$\Psi^S_t = \frac{\partial \hat{V}^S_{t+1}}{\partial S_{t+1}}\frac{\partial S_{t+1}}{\partial x^S_{s,t}} + \frac{\partial \hat{V}^S_{t+1}}{\partial I_{t+1}}\frac{\partial I_{t+1}}{\partial x^S_{s,t}} \tag{30}$$

$$\Psi^I_t = \frac{\partial \hat{V}^S_{t+1}}{\partial S_{t+1}}\frac{\partial S_{t+1}}{\partial x^I_{s,t}} + \frac{\partial \hat{V}^S_{t+1}}{\partial I_{t+1}}\frac{\partial I_{t+1}}{\partial x^I_{s,t}}. \tag{31}$$

Note that $-\frac{\partial S_{t+1}}{\partial x^S_{s,t}} = \frac{\partial I_{t+1}}{\partial x^S_{s,t}} = \frac{\partial p^P_t}{\partial x^S_{s,t}} S_t$ and $-\frac{\partial S_{t+1}}{\partial x^I_{s,t}} = \frac{\partial I_{t+1}}{\partial x^I_{s,t}} = \frac{\partial p^P_t}{\partial x^I_{s,t}} S_t$, so (29) becomes:

$$MRS^{SP}_{t,I,S} = \frac{\frac{\partial p^P_t}{\partial x^I_{s,t}}[V^I_{t+1} - V^S_{t+1} + (1 - p^P_t)(-\frac{\partial \hat{V}^S_{t+1}}{\partial S_{t+1}} S_t + \frac{\partial \hat{V}^S_{t+1}}{\partial I_{t+1}} S_t)]}{\frac{\partial p^P_t}{\partial x^S_{s,t}}[V^I_{t+1} - V^S_{t+1} + (1 - p^P_t)(-\frac{\partial \hat{V}^S_{t+1}}{\partial S_{t+1}} S_t + \frac{\partial \hat{V}^S_{t+1}}{\partial I_{t+1}} S_t)]} = \frac{\frac{\partial p^P_t}{\partial x^I_{s,t}}}{\frac{\partial p^P_t}{\partial x^S_{s,t}}}. \tag{32}$$

Under a lockdown policy that sets $p_t = p^P_t$, it follows that the marginal rate of substitution in (32) is equal to the one in (28).

B. First-Order Conditions of the Social Planner in the SIR-Network Model with Endogenous Cross-Links

The first-order conditions for the social planner's problem of the SIR-network model for the home activity of susceptible and infected individuals and recovered individuals' home and social activities are equivalent to those obtained under the decentralized equilibrium. For the levels of social activity of susceptible and infected individuals in each group j vis-à-vis each group k, $x_{s,t}^{S,jk}$ and $x_{s,t}^{I,jk}$, the first-order conditions are as follows:

$$S_t^j \frac{\partial U(x_{h,t}^{S,j}, x_{s,t}^{S,j})}{\partial x_{s,t}^{S,jk}} + \sum_n S_t^n \left\{ \beta \frac{\partial p^{Pn}(\cdot)}{\partial x_{s,t}^{S,jk}} (\hat{V}_{t+1}^{I,n} - \hat{V}_{t+1}^{S,n}) + \beta(1 - p_t^{Pn}(\cdot)) \sum_m \left[\frac{\partial \hat{V}_{t+1}^{S,n}}{\partial S_{t+1}^m} \frac{\partial S_{t+1}^m}{\partial x_{s,t}^{S,jk}} + \frac{\partial \hat{V}_{t+1}^{S,n}}{\partial I_{t+1}^m} \frac{\partial I_{t+1}^m}{\partial x_{s,t}^{S,jk}} \right] \right\} = 0 \tag{33}$$

$$I_t^j \frac{\partial U(x_{h,t}^{I,j}, x_{s,t}^{I,j})}{\partial x_{s,t}^{I,jk}} + \sum_n S_t^n \left\{ \beta \frac{\partial p^{Pn}(\cdot)}{\partial x_{s,t}^{I,jk}} (\hat{V}_{t+1}^{I,n} - \hat{V}_{t+1}^{S,n}) + \beta(1 - p_t^{Pn}(\cdot)) \sum_m \left[\frac{\partial \hat{V}_{t+1}^{S,n}}{\partial S_{t+1}^m} \frac{\partial S_{t+1}^m}{\partial x_{s,t}^{I,jk}} + \frac{\partial \hat{V}_{t+1}^{S,n}}{\partial I_{t+1}^m} \frac{\partial I_{t+1}^m}{\partial x_{s,t}^{I,jk}} \right] \right\} = 0, \tag{34}$$

where p_t^{Pn} is given by equation (21) and (the summations over) n and m refer to all groups, including j and k.

C. Additional Figures

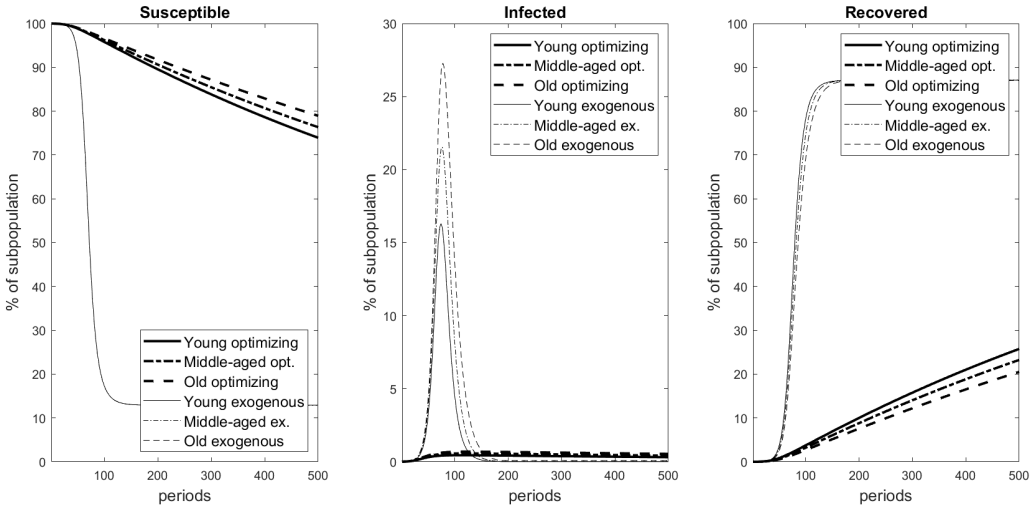

Figure 7
Comparison of SIR-Network Models with Endogenous Social Activity ($\delta = 0.5$) vs. Constant Exogenous Contact Rates

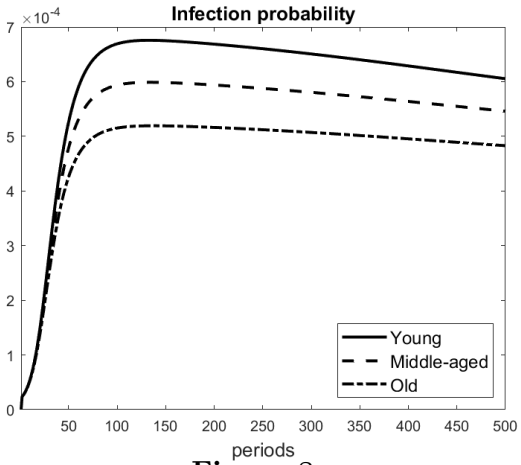

Figure 8
Dynamics of Infection Probabilities in the SIR-Network Model ($\delta = 0.5$)

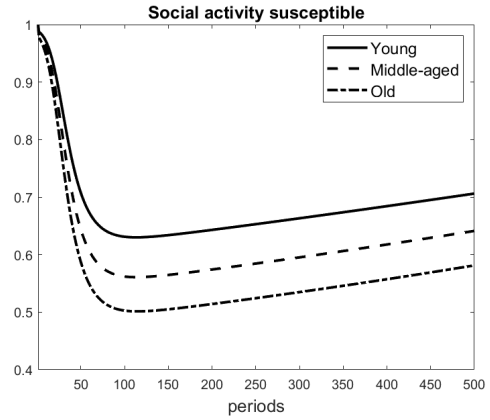

(a) $\delta = 0.5$

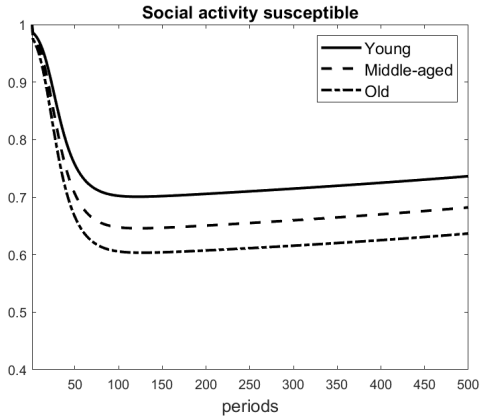

(b) $\delta = 1$

Figure 9
Aggregate Social Activity of Susceptible Young, Middle-aged, and Old Individuals with Different Degrees of Altruism in the SIR-Network Model

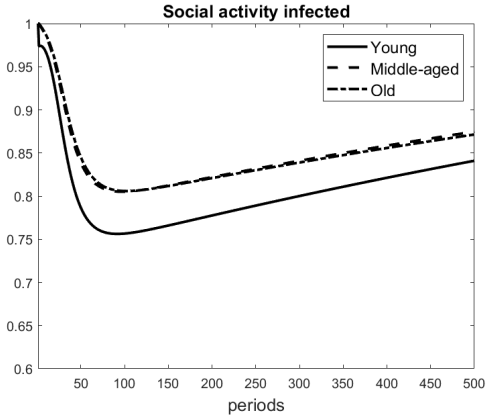

(a) $\delta = 0.5$

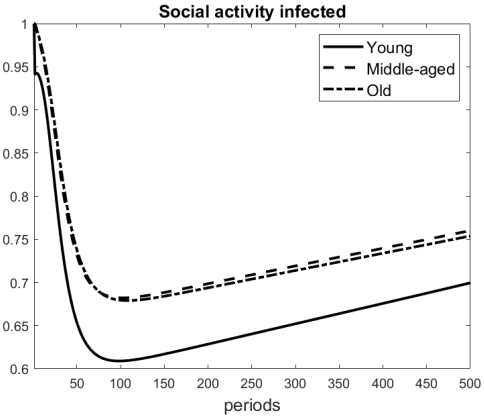

(b) $\delta = 1$

Figure 10
Aggregate Social Activity of Infected Young, Middle-aged, and Old Individuals with Different Degrees of Altruism in the SIR-Network Model

D. Details for the Simulations

The model equations of the baseline model that we use for the simulations are as follows:

$$S_{t+1} = S_t - p_t S_t - \epsilon \mathbb{1}_{t=1} \tag{A1}$$

$$I_{t+1} = I_t + p_t S_t - \gamma I_t + \epsilon \mathbb{1}_{t=1} \tag{A2}$$

$$R_{t+1} = R_t + \gamma I_t \tag{A3}$$

$$V_t^S = U(x_{h,t}^S, x_{s,t}^S) + \beta[p_t V_{t+1}^I + (1-p_t) V_{t+1}^S] \tag{A4}$$

$$V_t^I = U(x_{h,t}^I, x_{s,t}^I) - C_t^I + \beta[(1-\gamma) V_{t+1}^I + \gamma V_{t+1}^R] + \delta S_t V_t^S \tag{A5}$$

$$V_t^R = U(x_{h,t}^R, x_{s,t}^R) + \beta V_{t+1}^R \tag{A6}$$

$$p_t(\cdot) = \eta x_{s,t}^S x_{s,t}^I (\bar{x}_{s,t})^{\alpha-1} I_t \tag{A7}$$

$$\frac{\partial U(x_{h,t}^S, x_{s,t}^S)}{\partial x_{s,t}^S} = \beta \eta x_{s,t}^I (\bar{x}_{s,t})^{\alpha-1} I_t (V_{t+1}^S - V_{t+1}^I) \tag{A8}$$

$$\frac{\partial U(x_{h,t}^I, x_{s,t}^I)}{\partial x_{s,t}^I} = \delta S_t \beta \eta x_{s,t}^S (\bar{x}_{s,t})^{\alpha-1} I_t (V_{t+1}^S - V_{t+1}^I). \tag{A9}$$

Note that there are no equations for the social interactions of recovered agents and the home activities of all three classes of agents, since we assume for simplicity that they are not affected by the evolution of the pandemic.

The model simulations are performed with Dynare 5.1. Initially, the economy is in a steady state and hit by a zero-probability MIT shock, increasing the total share of infected agents from 0 to ϵ. There are no other aggregate shocks, so that we can compute a perfect-foresight solution. The default algorithm is the Newton method. Depending on the parameters and the model variant, in some cases the Newton method cannot solve the problem. In such cases, a homotopy technique is used to divide the problem into smaller steps. Specifically, the size of the shock is initially diminished, and the problems are solved iteratively, progressively increasing the shock size until the problem converges.

We use this algorithm for the simulations at hand since, first, it is a fully non-linear algorithm, allowing to account for the non-linearity that the infection probabilities bring to

the SIR system. Second, our model is in discrete time, which helps to specify future variables fully, and the algorithm is well-suited for discrete-time models.

E. Limitations of the Homogeneous SIR and SIR-Network Models with Non-Optimizing Agents

In the basic homogeneous SIR model (see Kermack and McKendrick, 1927; or, more recently, Hethcote, 2000), there are three classes of agents: susceptible (S), infected (I), and recovered (R). The number of susceptible individuals decreases as they become infected. At the same time, the number of infected individuals increases by the same amount, but also declines because people recover. Recovered people are immune to the disease and, thus, stay recovered. The mathematical representation of the model is as follows:

$$S_{t+1} = S_t - \lambda I_t S_t \tag{A10}$$

$$I_{t+1} = I_t + \lambda I_t S_t - \gamma I_t \tag{A11}$$

$$R_{t+1} = R_t + \gamma I_t, \tag{A12}$$

where $N_t = S_t + I_t + R_t$ is the overall population and λ is the transmission rate of the infection.

Hence, $p_t = \lambda I_t$ is the probability that a susceptible individual becomes infected at time t. In the classical SIR model, the latter is assumed to be exogenous, constant, and homogeneous across groups. Even as agents become aware of the pandemic, it is assumed that they do not adjust their behavior. More recent versions of the SIR model incorporate the dependence of contact rates on the heterogeneous topology of the network of contacts and mobility of people across locations (see, for example, Pastor-Satorras and Vespignani, 2001a,b). Other variants of the model incorporate the dependence of infection rates on the activity intensity of each node of the network (see Perra et al., 2012, for solving an activity-driven SIR model using mean-field theory and Moinet et al., 2018, who introduce a parameter capturing an exogenous decay of the infection risk due to precautionary behavior).

In all of these instances, however, the model's infection probability is introduced in an ad-hoc fashion and immutable over time. Overall, those relations give a naïve representation of human behavior and are, thus, subject to the Lucas critique. This is a crucial shortcoming,

particularly if one intends to apply those models to optimal policy design. Indeed, assuming that agents do not change their behavior (here: their social interactions) in their best interest in response to the shocks (here: the infection shock) and to the policy itself leads to misguided policy prescriptions. Therefore, developing a sound model for the prediction of disease diffusion is ultimately crucial for the effectiveness of containment policies.

F. SIR-Network Model with Optimizing Agents and Fixed Cross-Group Contact Rates

In this section, we present a network model in which different groups choose the general level of social activity, but the cross-group contact rates are exogenous and heterogeneous. The exogenous intensity of these contacts across groups can be characterized by the degree of homophily.[22] If two groups have lower homophily and, hence, have more frequent contact with other groups, they will internalize their relative risk of infection. The groups in the community could correspond to, e.g., the age structure, different strengths in ties, or closer face-to-face interactions in the workplace. The underlying idea is that contact rates tend to be higher among peer groups.

Consider a population with different groups $j = 1, ..., J$. The number of people in each group is N_j. Groups have different probabilities of encounters with the other groups. The contact intensity between group j and any group k is $\xi_{j,k}$. How fast the outbreak then spreads to the rest of the network depends on the relative exposure of the initially infected group to the other groups. Each susceptible individual of group j experiences a certain number of contacts per social activity with infected individuals of her own group, but also of the other groups. The number of contacts experienced by group j depends on the average level of social activity in each group k weighted by the contact intensity across groups, and is equal to: $m^j(\hat{x}^j_{s,t}) = \left(\sum_k \xi_{j,k}(\bar{x}^{S,k}_{s,t} S^k_t + \bar{x}^{I,k}_{s,t} I^k_t + \bar{x}^{R,k}_{s,t} R^k_t)\right)^{\alpha}$.

The probability of infection of a susceptible person in group j is modified as follows: $p^j_t(\cdot) = \eta x^{S,j}_{s,t} \sum_k \left[\xi_{j,k} x^{I,k}_{s,t} \frac{m^j(\hat{x}^j_{s,t})}{\hat{x}^j_{s,t}} I^k_t\right]$, where $k = 1, .., J$ and $\xi_{j,j} = 1$. The probability of meeting an infected person from any other group k is weighted by the likelihood of the contacts across groups, $\xi_{j,k}$. As before, atomistic individuals take the average social activity

22 It describes "the tendency of various types of individuals to associate with others who are similar to themselves" (Currarini et al., 2009). See also Fehr and Schmidt (1999) or Fehr and Gächter (2000).

and the average social encounters as given. The first-order condition for the level of social activity of susceptible individuals belonging to group j now reads as follows:

$$\frac{\partial U(x_{h,t}^{S,j}, x_{s,t}^{S,j})}{\partial x_{s,t}^{S,j}} + \beta\eta \sum_k \xi_{j,k} x_{s,t}^{I,k} \frac{m^j(\hat{x}_{s,t}^j)}{\hat{x}_{s,t}^j} I_t^k (V_{t+1}^{I,j} - V_{t+1}^{S,j}) = 0. \tag{A13}$$

We can now derive the first-order condition for the level of social activity of infected individuals belonging to group j:

$$\frac{\partial U(x_{h,t}^{I,j}, x_{s,t}^{I,j})}{\partial x_{s,t}^{I,j}} + \delta\beta\eta \sum_k \frac{S_t^k}{N_t^k} \xi_{k,j} x_{s,t}^{S,k} \frac{m^k(\hat{x}_{s,t}^k)}{\hat{x}_{s,t}^k} I_t^j (V_{t+1}^{I,k} - V_{t+1}^{S,k}) = 0, \tag{A14}$$

where infected individuals internalize the impact of their choices on all three groups, weighted by their respective shares S_t^k/N_t^k. The first-order conditions for the recovered individuals remain the same as in the baseline model, but now there is one for each group j.